EFFECT OF PROCESSING DEFICIENCIES ON VACUUM-BAG-ONLY COMPLEX-SHAPE PREPREG LAMINATE CONSOLIDATION AND INTERLAMINAR TENSILE BEHAVIOUR

Nicolas Krumenacker and Pascal Hubert

Department of Mechanical Engineering, McGill University
817 Sherbrooke St W, Montreal, Quebec, Canada, H3C 0C3
Email: nicolas.krumenacker@mail.mcgill.ca, pascal.hubert@mcgill.ca
Web page: http://composite.mcgill.ca/

Keywords: Vacuum-bag-only, out-of-autoclave, complex-shape laminate, curved beam strength.

ABSTRACT

High-quality flat composite parts can now be readily manufactured via out-of-autoclave prepregs and vacuum-bag-only processing. Still, the aim of these technologies remains the robust manufacturing of large complex parts such as primary aerospace structures. The key challenge remains the inherent variability observed in cured complex-shape regions that primordially exhibit severe thickness variations and porosity.

A right-angle corner geometry is chosen as a representative complex-shape laminate case and was limited to convex corners only. The current work investigates the relationship between fibre architecture, local thickness deviation and macro-porosity, and interlaminar tensile behaviour for several commonly encountered process conditions. Corner thickening and void morphology are quantified via a novel thickness profile measurement approach in Matlab and micro-CT scans respectively. In turn, these findings are correlated to interlaminar tensile behaviour via curved beam strength testing (ASTM D6415).

Results indicate that processing deficiencies do not appear to significantly influence convex corner thickening, which is primarily driven by inter-ply friction; however, they do lower curved beam strength given higher observed porosity. Of particular note, UD fibre architecture was markedly more affected by processing deficiencies indicating a lower propensity to impede delamination compared to woven architectures.

1 INTRODUCTION

1.1 Background and motivation

Curing in industrial autoclaves remains the preferred processing route for the majority of high-performance, advanced thermoset composite applications. For one, primary aerospace structures require excellent laminate consolidation and often complex geometric designs (e.g. corners and ply-drops) that can currently only be readily achieved via autoclave curing. High consolidation pressure (>> 1 atm) translates into high hydrostatic resin pressure during resin impregnation and gelation that effectively supresses void formation—one of the most consequential types of defects affecting the mechanical strength and delamination resistance of composite laminates. Autoclave curing thus remains the benchmark process against which other processes are measured [1].

That being the case, demand for ever larger and complex parts across industries is rapidly exacerbating the capacity of current autoclave infrastructure and equipment. Upfront capital investment and operating costs are steeply rising, as autoclaves are scaled-up to keep up with demand. Meanwhile, production is adversely affected, and the rates of composite insertion and innovation in industry may in turn suffer. One incentive across industries to circumvent these impediments is to shift away from autoclave curing and towards more energy-efficient, out-of-autoclave (OOA) vacuum-bag-only (VBO) processes and dedicated prepregs. These technologies aim to deliver the same level of

quality and performance as their autoclave counterparts, while significantly lowering equipment and operating costs, improving energy efficiency, and streamlining production [2-4].

High-quality, flat composite laminates can already be readily achieved via VBO processes thanks to advances in dedicated prepregs that feature improved air-evacuation and optimized resin chemistry [5-9]. More recently, such processes have been used to cure a select few aircraft parts of increasing size, complexity, and structural importance [4, 9, 10]. Despite this recent progress, the key challenge for OOA/VBO technologies remains the inherent variability observed in cured complex-shape regions (e.g. corners) that primarily exhibit significant local thickness deviation and porosity, as well as in- and out-of-plane fibre waviness. The accelerated insertion of these technologies in high-end industries hinges on a deeper understanding of the influence of processing parameters on laminate consolidation and mechanical performance in complex-shape laminates. In addition, the development of robust predictive tools that can accurately predict thickness deviation porosity and their combined effect on mechanical performance will further help to bolster industry confidence in and acceptance of these developing technologies.

1.2 Literature survey

A decent understanding of the compaction of complex-shape laminates exists in the literature stemming from lab-scale studies that have been mostly conducted on autoclave-cured laminates [11-13], and to a lesser extent on VBO-cured laminates [14-19]. All studies irrespective of the chosen process have observed local thickness deviation in complex-shape regions: thickening is prevalent in most cases over both convex and concave tool features; in turn, thinning occurs only over convex tool features and given specific fibre orientation (i.e. normal to the gradient) and resin bleeding conditions.

Hubert and Poursartip first offered a fundamental explanation for this local thickness deviation [20]. In order to satisfy force equilibrium in complex-shape regions, the tool-side reaction and bag-side applied pressures must differ given that the local tool and vacuum bag surface areas likewise differ. The resulting consolidation pressure differential in complex-shape regions induces a local thickness deviation from that induced in flat regions. Brilliant and Hubert proposed a model based on this explanation to predict the thickness deviation in VBO-cured right-angle corner laminates [14]. The model assumes inter-ply slippage during compaction and resin impregnation and accounts for the prepreg bulk factor, though it fails to account for inter-ply friction and other phenomena that may impede compaction. Levy et al. proposed a subsequent model that incorporates inter-ply friction and highlighted two overarching mechanisms that drive local thickness deviation: a) reduction in consolidation pressure due to inter-ply slippage as originally proposed by Hubert and Poursartip, and b) geometric constraint when ply slippage does not occur [18]. Further work is required to better understand and capture additional effects such as operator-induced variability, which may have a large impact on lab-scale experimental data as VBO-cured laminates are typically manually laid-up and vacuum-bagged. Besides thickness deviation, it should also be emphasized that local reductions in consolidation pressure will result in higher porosity and thus poorer matrix-dominated properties.

Whereas both autoclave- and VBO-cured complex-shape laminates exhibit local thickness variation, OOA prepregs are prone to greater deviations due to their generally much larger bulk factors. They are only partially impregnated and contain a dry fibre mid-plane region in the case of unidirectional tape and dry intra-tow channels in the case of bidirectional woven architectures. These dry regions are designed to maximize air-evacuation during laminate compaction and resin impregnation [5, 6, 9]. A large thickness reduction thus occurs during the laminate compaction and resin impregnation phases of the cure. This “de-bulking” can have a drastic impact on local thickness deviation in the common occurrence that inter-ply slippage is restricted, in which case fibre bridging will ensue over concave tool features and fibre compression and waviness will ensue over convex tool regions [14]. In addition, the limited consolidation pressure in VBO processes ($\leq$ 1 atm) amplifies the effect that other processing parameters can have [16]. The high consolidation pressure present in the case of autoclave curing would otherwise suppress such effects. Hence, higher prepreg bulk factors and limited consolidation pressure are expected to increase local thickness deviation in VBO-cured complex-shape laminates compared to similar autoclave-cured laminates.

Of particular importance to the following work, Centea and Hubert investigated the effect of process deficiencies on VBO-cured flat laminates consisting of OOA unidirectional tape and two bidirectional woven prepregs [16]. Reductions in consolidation pressure as a result of deficient atmospheric pressure and partial vacuum pressure losses, as well as entrapped air due to restricted air-evacuation all resulted in significantly higher void contents for the tested woven laminates; however, the superior air-evacuation properties of the tested unidirectional tape resulted in acceptable porosity levels in all but the restricted air-evacuation case. These findings were correlated with observed micro- and macro-void concentrations and morphologies. Similar work has yet to be conducted on VBO-cured complex-shape laminates, for which it is expected that process deficiencies will have a similar yet more pronounced effect given the often already deficient local consolidation pressure.

Lastly, the flexural response of curved laminates has been thoroughly investigated in the literature mainly for autoclave-cured curved laminates. Reduction of mechanical testing data is mainly based on Lekhnitskii's anisotropic curved beam theory [21]. Kedward et al. presented an early review the links between premature failure of complex-shape hardware parts and localized curvature effects and proposed approximate testing methods to predict the interlaminar tensile behaviour [22]. Cui et al. later presented a thorough review of interlaminar tensile strength (ILTS) testing methods and first proposed the use of a simpler curved beam specimen loaded under four-point bending [23]. This test method effectively laid the groundwork for the ASTM D6415 curved beam strength (CBS) testing standard used in this work [24]. Much more recently, Seon et al. proposed further developed the CBS method in order to generate much more accurate ILTS properties with significantly reduced data scatter, which is notable setback of the standardized CBS method. Of greater pertinence to the scope of the proposed work, Cui et al. proposed guideline for CBS specimen design and provide a throrough of the test theory and test data reduction [23]. In addition, Seon et al. provide relevant insights into the effect of porosity on measured properties and data scatter.

1.3 Objective and overview

The following work investigates the effect of process deficiencies on the consolidation, local laminate quality, and interlaminar tensile behaviour of VBO-cured complex-shape laminates that consist of OOA unidirectional tape and two bidirectional woven prepregs. A 90° V-shape (corner) sample geometry is chosen as a representative complex-shape laminate case. In addition, the samples presented in this work have all been processed on a convex tool; concave specimens are also of high interest and will be investigated in subsequent works. The first part of the current work aims to generate full cross-sectional thickness profiles for each sample to more accurately and precisely determine corner thickness deviation. These findings are then correlated with micro-CT scans of selected corner regions to assess the local laminate quality in terms of macro-porosity. In the second part, curved beam strengths are obtained via mechanical testing for each sample and correlated with corner thickness deviation and porosity.

2 METHODOLOGY AND EXPERIMENTAL PROCEDURES

2.1 Selected materials and processing conditions

The three OOA prepregs that are investigated in this work are all comprised of Cytec Cycom® 5320 epoxy resin that is b-staged and partially impregnated in Cytec Thornel® T650/35 continuous carbon fibre reinforcements. Table 1 summarizes the specifications of the three selected fibre architectures: unidirectional tape (UD), plain weave (PW), and 8-harness satin weave (8HS). The nominal laminate thickness for all manufactured laminates is approximately 4.21 ± 0.02 mm, which matches the nominal thickness prescribed in ASTM D6415 in the special case of interlaminar tensile strength (ILTS) testing [24]. The laminate stacking sequences designed to achieve this nominal thickness are included in Table 1, with the 0° ply orientation pointing in the corner hoop direction. In addition, the nominal convex tool corner radius is approximately 5.91 ± 0.08 mm. This radius along with the nominal laminate thickness are both chosen to favour delamination failure in the corner under

four-point bending, as opposed to tensile or compressive fibre failure in the corner due to bending or interlaminar shear failure in the flanges [23].

Table 1 – Selected fibre architecture specifications.

Designation	Fibre architecture (filaments per tow)	Areal weight (g/m^2)	Resin content (%)	Laminate stacking sequence
UD	Unidirectional tape (NA)	145	33	$[0]_{30}$
PW	Plain weave (3k)	196	36	$[0]_{21}$
8HS	8-harness sating (3k)	370	36	$[0]_{11}$

Three processing conditions detailed in Table 2 are additionally investigated for each of the three fibre architectures, resulting in a total of nine samples (i.e. UD-B H and R, PW-B, H and R, and 8HS-B, H, and R). First the baseline condition (B) is representative of near-optimal processing conditions and sets a benchmark, against which the two selected processing deficiencies can be compared. Second the half vacuum-bag pressure loss condition (H) is representative of a very deficient consolidation pressure. Third and last, the restricted air-evacuation condition (R) is representative of the curing of large-scale laminates on the order of several meters or more such as primary aerospace structures. OOA prepregs are designed to be much more air permeable in-plane than through-the-thickness, most notably in the case of UD tape. Large-scale laminates therefore have a propensity to trap air at their center as air-evacuation distance increases, which is of great research interest.

Table 2 – Selected processing conditions.

Designation	Process condition	Vacuum bag pressure (atm)	Air-evacuation	De-bulk steps	Room-temp. Hold
B	Baseline	~1 atm	Edge-only	5 min/ply	12 hr
H	Half-vacuum loss	~0.5 atm	Edge-only	5 min/ply	12 hr
R	Restricted air-evacuation	~ 1 atm	Restricted	None	None

2.2 Layup, processing and specimen machining

Preparation: The laminates are manually laid-up and vacuum-bagged following the vacuum-bagging consumables sequence illustrated in Figure 1. The aluminum tool surface is first treated with a solvent-based tool sealer followed by a solvent-free semi-permanent release agent (Zyvax® Sealer GP and EnviroShield, respectively). Release agent is used instead non-perforated release film in order to better fix the first ply to the tool surface and to prohibit the possible transfer of wrinkles onto the laminate's inner corner surface. That being the case, narrow strips of non-perforated release film (Airtech A4000) are placed under the laminate edges in order to prevent local roughing of the released tool surface during de-bulking, which increases the likelihood of post-cure tool-part adherence.

Layup: Plies measuring 55 by 25 cm are laid up according to the respective laminate stacking sequences (Table 1). A de-bulk step of 5 min is applied between each ply layup to improve consolidation, except for the restricted air-evacuation sample. Edge breathing is achieved via dry fiberglass tape wrapped around sealant tape (Airtech GS-213-3) and placed around the laminate edges, while restricted air-evacuation is achieved by using sealant tape only to seal the edges. A layer of non-perforated release film is then placed over the laminate to prohibit resin bleeding into the breather layers and to better seal the laminate in the case of restricted air-evacuation. The breather layer consists principally of a fiberglass, plain-weave peel ply instead of a standard polyester breather in order to reduce the bulk of bagging consumables and mitigate the possible formation of wrinkles on the outer laminate surface during de-bulking. Breather strips (Airtech Airweave® N4) are also used around the laminate edges to create a supplemental air-evacuation channel leading to the vacuum ports. Lastly, the top surface of the mould is sealed with a standard nylon vacuum-bagging film (Airtech Wrightlon® 6400) and sealant tape around the edges of the tool surface.

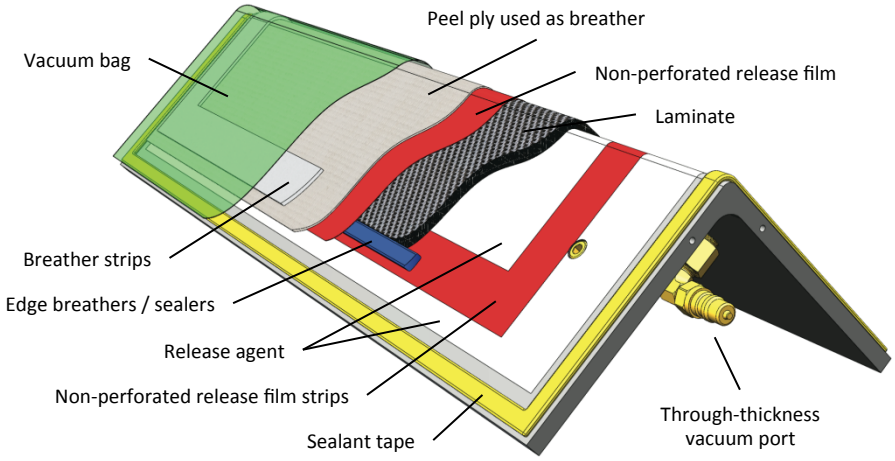

Figure 1 – Schematic of the vacuum-bagging consumables sequence on the convex aluminum tool.

Cure cycle: The baseline and half-vacuum loss laminates are first held for 12 hr at room temperature under full vacuum and half-vacuum, respectively, in order to allow for maximum evacuation of entrapped air. The laminates are subsequently cured in a regular Blue M lab convection oven. The cure cycle is optimized using the cure kinetic model developed by Kratz et al. for Cytec Cycom® 5320 [25]. It consists of the following stages: i) curing at 120 °C for 2 hr with a heat ramp of 2 °C/min, ii) air cooling to RT and part removal from the tool, iii) post-curing at 180 °C with a heat ramp of 2 °C/min, and iv) final air cooling to RT. The laminates are post-cured freestanding in order to minimize cure-stresses induced by the mismatch in CTEs between the aluminum tool and composite laminate. The vacuum bag pressure and laminate-tool interface temperature are monitored to ensure that no undesirable process deviations occur. The final degree of cure is estimated at 98.5 % for all laminates based on the cure cycle and cure kinetics model.

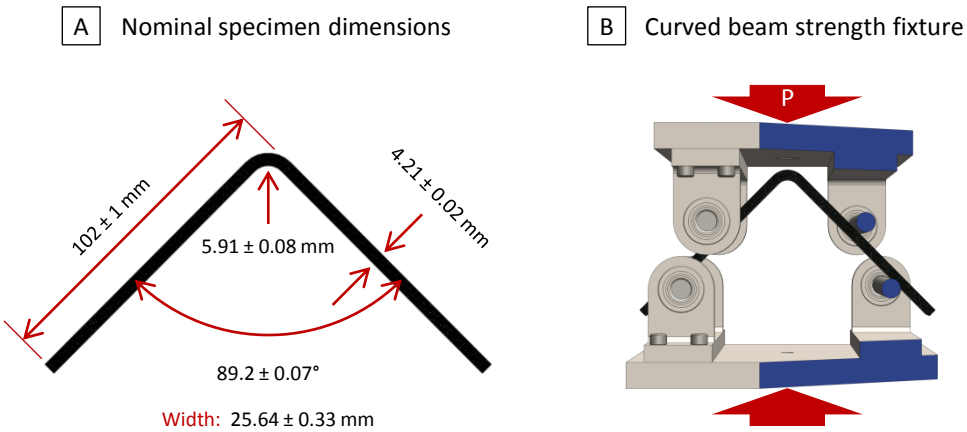

Figure 2 – Schematics of the A) nominal corner specimen dimensions and B) the curved beam strength fixture (ASTM D6415) with a loaded specimen (the fixture is partially sectioned-off in blue to more clearly show roller-specimen contact).

Specimen machining: Corner specimens are cut from each sample corner plate with a water-lubricated, circular diamond saw fitted with a polymer matrix composite-specific wafer diamond blade. Painstaking care is taken to impart as little machining-induced damage to the corner regions. Poor machined-edge quality is directly can lead to reductions in interlaminar strength properties and large corresponding data scatters [24, 26]. The specimens are then hand finely ground on a polishing machine up to a diamond grit of 1200 (Struers MD-Piano^{TM} discs) in order to remove the majority of remaining machining artefacts (i.e. microscopic surfaces notches). The nominal specimen dimensions are given in Figure 2A and adhere to those prescribed in ASTM D6415 [24]. Of the multiple

specimens cut per sample beam, five specimens are reserved for dimensional analysis and subsequent mechanical testing, and an additional specimen is reserved to conduct a representative corner laminate quality assessment (micro-CT).

2.3 Corner consolidation and porosity assessment

Corner specimens destined for mechanical testing are scanned at high resolution (> 1500 dpi) on a standard Canon home-office scanner; all specimens of a given sample are scanned together. A custom Matlab code was developed to process the scanned images, recognise and segment the various corners in each image, and effectively detect the convex and concave edges of each corner for subsequent analysis. The output is a mean (or average) thickness profile for each sample as a function of the concave, tool-side edge, which is designated as the reference edge for convex corners. In addition, the code computes the dimensions necessary for the analysis of curved beam strength (CBS) mechanical testing data as well as the mean percent corner thickness deviation for each sample. Besides obvious practical reasons, the true benefits of this dimensional analysis tool are i) to remove human error from thickness measurements—particularly in the corner, and ii) to generate a complete thickness profiles in the corner regions as opposed to relying on micrometer point measurements.

A select few specimens are additionally analyzed via high-resolution x-ray micro-computed tomography (micro-CT) using a Skyscan 1172 High Resolution micro-CT unit in order to complement the above thickness deviation analysis and examine the local laminate quality in terms of local macro-porosity at corners. The selected specimens are trimmed (25 mm flange length and 18 mm width) using a lab-scale Struers precision lab-bench saw fitted with a composite-specific diamond precision cut-off blade. The trimmed section are then x-rayed over a 180° span at 0.28° intervals with the following radiographic parameters: no filter, voltage source of 40 kV, intensity of 250 μA intensity, image size of 4000 x 2096 pixels, and pixel resolution of 4.96 μm. The x-ray images are reconstructed in 3D using equipment-specific software for post-analysis and viewing. It should be noted that it is impractical to visualize micro-voids and to calculate accurate void contents given current equipment and protocol limitations. Nevertheless, pertinent qualitative insights may still be drawn for estimating the extent of macro-porosity.

2.4 Curved beam strength testing

ASTM D6415 mechanical testing standard is selected to assess the effect of processing deficiencies on the interlaminar tensile behaviour of the corner specimens. This standard is one of the few recognized standards to be devised specifically for the mechanical testing of corner laminates. One of the clear advantages is that the corners are loaded under four-point bending with no end-loading. A pure bending moment is generated in the corner that results in a simpler stress state with no interlaminar shear. In addition, the pure bending moment induces an interlaminar tensile stress that is nearly twice that induced by an equivalent end-load [23]. A second advantage is the ease and speed of testing. The general property generated by this test and used in this work is the curved beam strength (CBS), which is “the moment per unit width (M/w) applied to the curved test section that causes a sharp decrease in applied load or delamination(s) to form” [24].

Mechanical testing is conducted on a MTS Insight electromechanical testing frame equipped with a 5 kN load cell. Corner specimens are placed in the standard CBS fixture build by Wyoming Test Fixtures Inc. specifically for ASTM D6415, as illustrated in Figure 2B. A loading rate of 1 mm/min is applied (twice the prescribed rate) in order to ensure specimen failure within 10 min. The curved beam strength is then calculated for each specimen per the standard at the last data point preceding the first load drop. The mean CBS is finally calculated for each sample. To complement the mechanical testing, one failed specimen is selected per sample that exhibits a representative overall failure mode. Each selected specimen is photographed at higher magnification using a Dino-Lite Edge portable digital microscope to reveal the extent of delamination. A small vice is used to slightly bend the open the specimen angle in order to render the delamination(s) more visible.

3 RESULTS AND DISCUSSION

3.1 Laminate corner consolidation and porosity results.

The generated thickness profiles are plotted and grouped by fibre architecture in Figure 3A-C. In addition, the calculated average percent corner thickening and thickness measurements for each sample and plotted for comparison in Figure 3D-E. Corner thickening occurred in all samples and is partly driven by the friction-thickening mechanism discussed by Levy et al. [18]. The normal bag-side applied pressure during de-bulking and curing combined with a relatively long flange length of roughly 125 mm effectively restricted inter-ply slippage and thus impeded consolidation. In addition, Melanie and Hubert observed that the application of edge breathers—and by extension edge-sealers—at the flange laminate edges directly impedes ply-slippage and induces in an even higher compressive hoop stress in the fibres [14]. In addition, the presence of corner thickening up to and beyond the corner inflection points (or shoulders) for all three UD thickness profiles (Figure 3A) is further indicative of the friction-thickening being in effect. A higher consolidation pressure should theoretically exist over convex tool features provided that inter-ply slippage is not impeded [20]. In contrast to woven laminates, the lower bulk factor of UD tape and relative flexibility and mobility of individual fibres allow for fibre waviness and thickening at the corner shoulders.

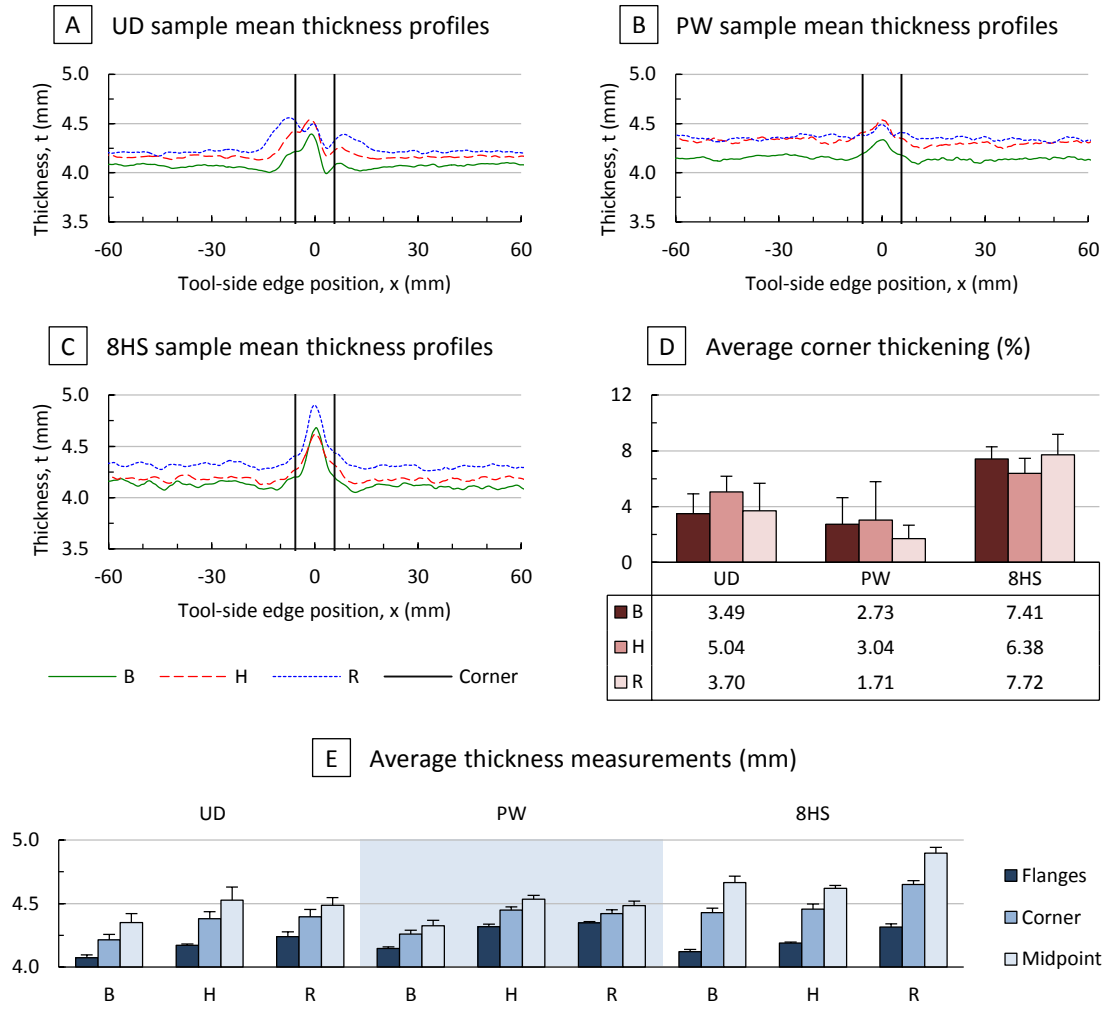

Figure 3 – Dimensional analysis results: mean thickness profiles of the A) UD, B) PW, and C) 8HS samples; D) Comparison of the average percent corner thickening per sample; and E) average flanges, corner and corner midpoint thickness measurements per sample.

Restricted air-evacuation proved to be the worse of the two selected deficient processing conditions, as it resulted in thicker flanges compared to half-vacuum loss (Figure 3E). In turn, the baseline processing condition resulted in consistently thinner flanges for all samples. This result agrees with the work conducted by Centea and Hubert on VBO-cured flat plates [16]. In turn, no clear trend was observed in the corner regions given the overlapping standard deviation ranges of the percent corner thickening data presented in Figure 3D. In fact, it may be noted that corner thickening does not seem to be significantly affected by the two selected deficient processing conditions in the case of convex corner laminates. It would be of great interest to determine if this observation holds true in the case of concave corner laminates.

Only one representative specimen was selected for each of the six baseline and half-vacuum loss samples, which are of greater interest than the restricted air-evacuation processing condition. Based on Centea and Hubert's finding for VBO-cured flat laminates [16], it is expected that greater differences in compaction, void morphology, and hence mechanical performance at the corner will exist between the baseline and half-vacuum loss processing conditions.

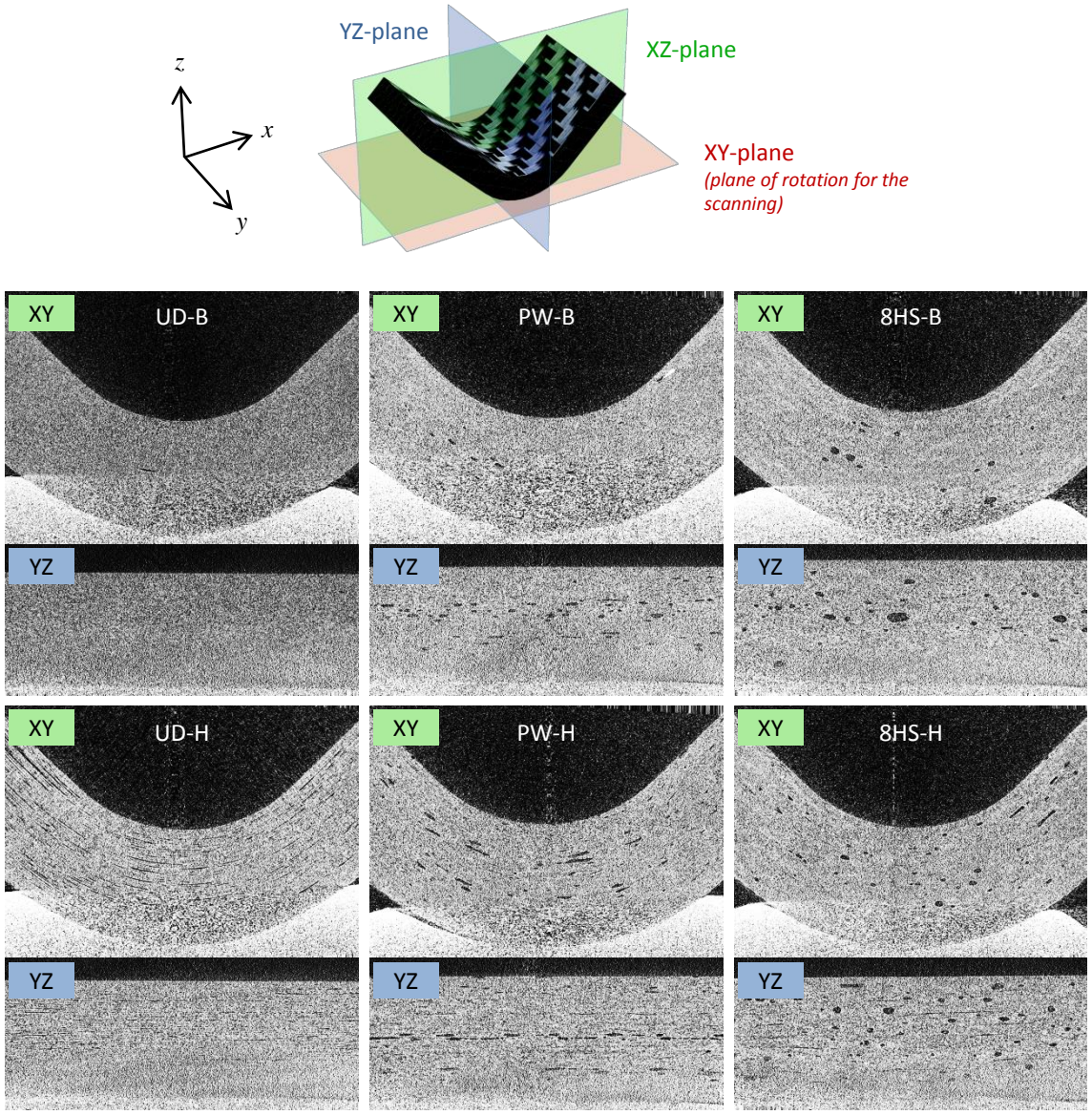

Figure 4 – Micro-CT results: section images in the corner hoop plane (XY) and in the radial-beam axis plane (YZ) for baseline and half-vacuum loss samples.

Cross-sectional images in the XZ and YZ planes were taken of the reconstructed 3D datasets for each representative specimen of interest and are presented in Figure 4. Macro-voids are the most prevalent observable type of defect. Irrespective of fibre architecture, higher macro-porosity can be observed for the half-vacuum loss specimens. That being the case, the UD baseline specimen exhibits negligible porosity in contrast to the corresponding PW and 8HS specimens. As was previously mentioned, the in-plane breathability of OOA-UD tape is significantly greater than that of its woven counterparts. In turn, voids appear to be stochastically dispersed throughout the thickness in all specimens with a generally greater distribution, except for the UD half-vacuum loss specimen. The latter is marked by pronounced macro-voids in the corner shoulders, which correlates with the corner shoulder thickening observed in UD thickness profiles. Lastly, it is apparent that fibre architecture clearly affects void morphology: macro-voids found in the UD specimens are characterized by comparatively much larger aspect ratios and are much thinner through-the-thickness, whereas macro voids found in the PW and 8HS specimens respectively increase in sphericity. Lastly, it is expected that the possibility of there being a void in the near vicinity of the maximum radial (or interlaminar tensile) stress location in the corner will significantly lower the measured strength values and scatter in data as noted by Seon et al. [26].

3.2 Curved beam strength testing results

Load vs. displacement curves are plotted and grouped by fibre architecture in Figure 5A-C, and the average CBS values are plotted for comparison in Figure 5D. All specimens failed, as intended, by mode of corner delamination. Load curves all exhibit an initial load drop indicative of the onset of delamination. Smaller drops follow this initial drop as new delaminations appear and existing delaminations grow unstable. The failure behaviour is otherwise progressive and indicative of stable delamination growth.

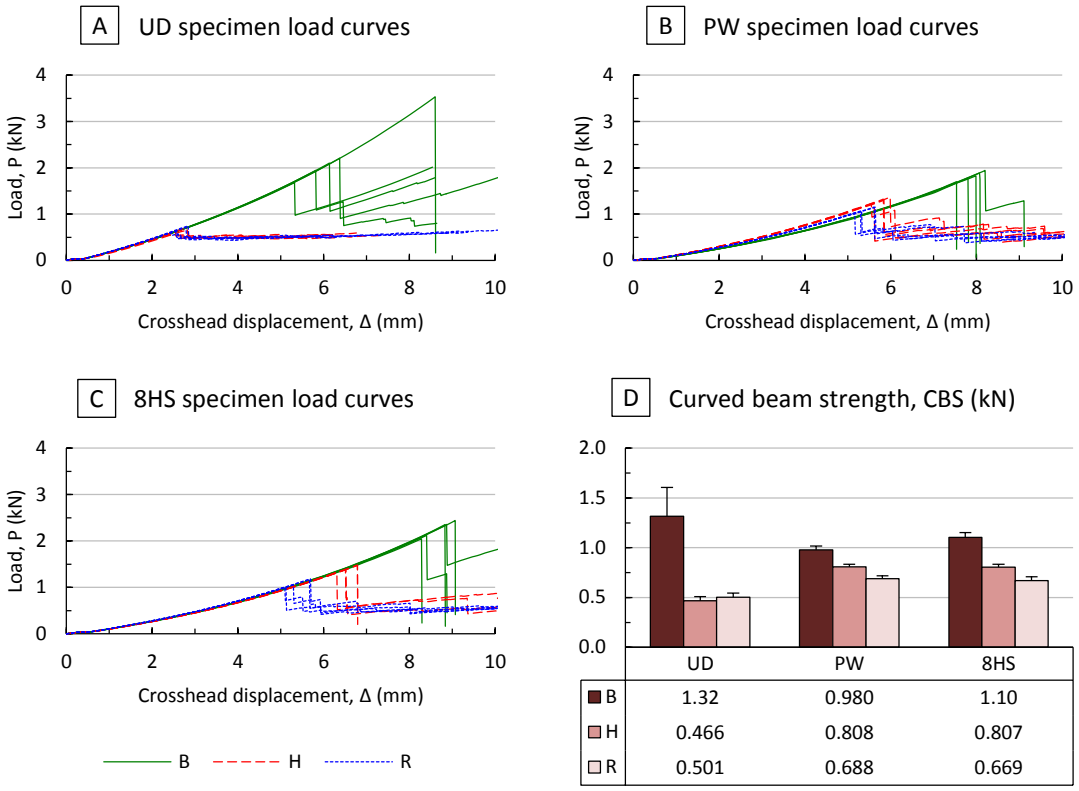

Figure 5 – Curved beam strength testing results: Load vs. crosshead displacement curves A) UD, B) PW, and C) 8HS specimens; and D) comparison of average sample curved beam strengths.

The UD baseline sample expectedly achieved a superior average CBS than corresponding woven samples, albeit while exhibiting a much larger standard deviation. This scatter in data is attributed by Seon et al. to the probability of there being a key void present in the corner region of highest interlaminar stress [26]. As the consolidation and laminate quality reach optimal levels, this probability lowers significantly, which in turn renders the morphology and location of any one void that much more critical.

In turn, processing deficiencies resulted drops in CBS in, with restricted air-evacuation again being the worst case. Of notable exception, however, is first the lack of difference observed between the UD half-vacuum loss and restricted air-evacuation samples, and second the lower performance of both of these samples compared to their woven counter parts. These finding suggests that UD tape laminates are much more sensitive to the presence of macro-voids and in turn processing deficiencies than bidirectional woven laminates. Macro-voids are typically present at ply-interfaces, whereas micro-voids are predominantly present in intralaminar regions such as fibre-tow crossover points. The wavy surface topography of woven plies impedes crack growth in contrast to the flatter topography of UD plies. This behaviour is clearly observable in macro-images taken of representative failed specimens that are presented in Figure 6. Delamination paths exhibit visually less out-of-plane (or radial) undulation in the case of the representative UD specimens. Lastly, delaminations clearly intersect visible macro-voids that may have initiated them.

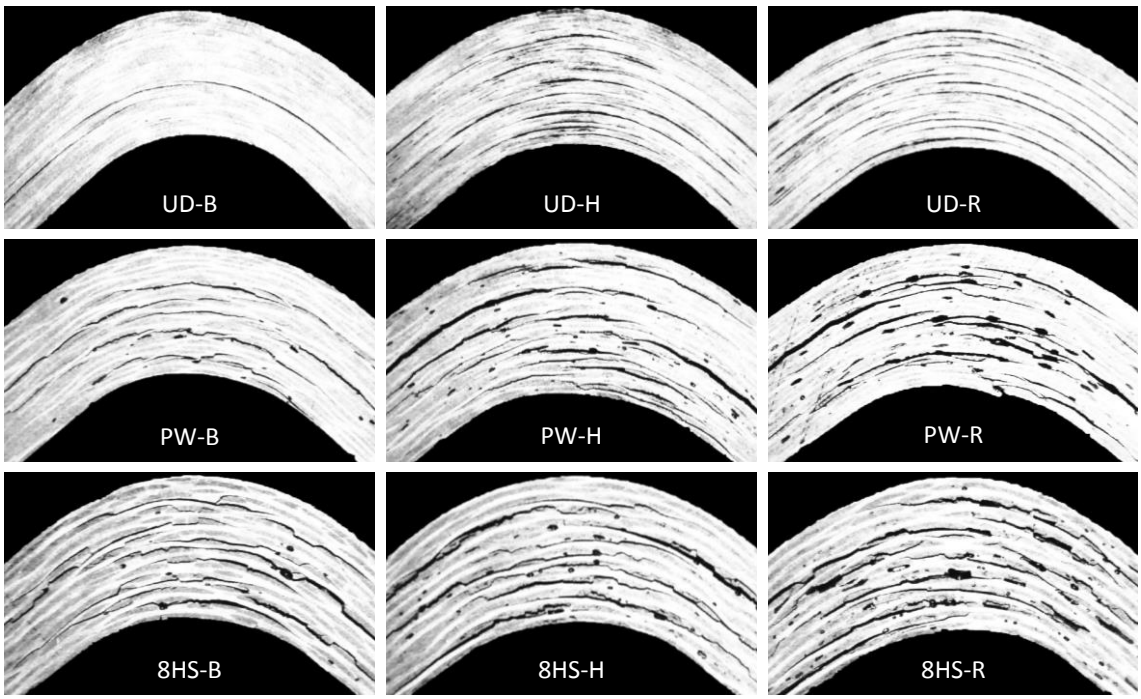

Figure 6 – Macro-images of representative failed specimens indicating corner delamination.

4 CONCLUSIONS

The present work investigated the effect of processing deficiencies on the corner consolidation and macro-porosity, and the curved beam strength of right-angle convex corner laminates that were produced via out-of-autoclave, vacuum-bag-only curing in a regular convection oven. Half vacuum-bag pressure loss and restricted air-evacuation were selected as representative, worse case processing deficiencies that can be encountered in industry, and compared to a near-optimal processing baseline. Test parameters also included three OOA prepregs with UD, PW, and 8HS fibre architectures

The generated thickness profiles corroborated the findings of Centea and Hubert for VBO-cured flat laminates [16], in that laminate thickness increased with decreasing consolidation pressure over the flanges and restricted air-evacuation proved to be the worse of the two selected processing

deficiencies. In contrast, processing deficiencies did not clearly affect corner thickness deviation. Corner thickening was observed in all cases and was primarily driven by inter-ply friction given a range of factors common to convex corner processing.

Of particular note regarding the thickness deviation analysis, scanned images of sample cross-sections were processed via a custom image processing and dimensional analysis code in order to generate full thickness profiles. This approach improved thickness measurement accuracy and precision by removing human error and refining measurements, in addition to generating a more comprehensive picture of local thickness variations and partly automating the measurement process.

In the second part of this work, processing deficiencies were shown to yield lower curved beam strengths (CBSs), with restricted air-evacuation again being the worst processing case. In turn, the UD tape was significantly more affected by processing deficiencies than the woven prepregs. The wavier surface topography of bidirectional woven prepregs was visually shown to impede delamination growth and lowered void-sensitivity in contrast to UD tape.

Lastly, UD laminates processed under the near-optimal baseline condition failed at a markedly higher CBS, though conversely resulted in much higher data scatter, which was linked to a lower probability in there being critical voids in the region of maximum radial stress [26]. Very large data scatter in CBS data (typically >> 10%) ultimately mitigates superior mechanical performance: larger knockdown factors are required, which can level performance across fibre architectures. This levelling in performance possibly renders woven prepregs potentially more attractive for use in complex-shape laminates, as secondary benefits (faster layup, improved draping-ability, etc.) take more precedence.

Overall, these conclusions bring additional clarity to the relationship between fibre architecture, local thickness deviation and macro-porosity, and interlaminar tensile behaviour for several commonly encountered process conditions. Of great future research interest will be the testing and analysis of similar concave laminates. The combined experimental data and observations will found the basis of future work on predictive thickness deviation and mechanical performance tools.

ACKNOWLEDGEMENTS

The authors would like to first and foremost acknowledge the in-kind contribution of Bombardier Aerospace in supplying OOA prepreg materials and vacuum-bagging consumables. Of equal importance is the financial support of: 1) the Natural Sciences and Engineering Research Council of Canada (NSERC) under the G8 Research Councils Initiative on Multilateral Research Fundin (grant: G8MUREFU2 – Material Efficiency, A First Step Toward Sustainable); and 2) the Centre de Recherche sur les Systèmes Polymères et Composites à Haute Performance (CREPEC). Last but not least, the authors wish to recognize the many members of the McGill Structures & Composite Materials Laboratory for their varied support.

REFERENCES

[1] P. Hubert, G. Fernlund and A. Poursartip, Autoclave processing for composites, in *Manufacturing techniques for polymer matrix composites (PMCs) (Eds. S.G. Advani and K.-T. Hsiao)*, Woohead Publishing Ltd., Cambridge, 2012, pp. 414-432.

[2] G. Gardiner, Out-of-autoclave prepregs: Hype or revolution? Oven-cured, vacuum-bagged prepregs show promise in production primary structures., *Composites World*, Gardner Business Media Inc., 2011, Cited May 13, 2015, Available: http://www.compositesworld.com/articles/out-of-autoclave-prepregs-hype-or-revolution.

[3] J. Schlimbach and A. Ogale, Out-of-autoclave curing process in polymer matrix composites, in *Manufacturing techniques for polymer matrix composites (PMCs) (Eds. S.G. Advani and K.-T. Hsiao)*, Woohead Publishing Ltd., Cambridge, 2012, pp. 435-481.

[4] R. Stewart, Carbon fibre market poised for expansion, *Reinforced Plastics*, **55**, 2011, pp. 26-31 (doi: doi:10.1016/S0034-3617(11)70216-8).

[5] L. Repecka and J. Boyd, Vacuum-bag-only-curable prepregs that produce void-free parts, Proceedings of the SAMPE 2002 47th International Symposium and Exhibition (Eds. B.M. Rasmussen, L. Pilato and H.S. Kliger), Long Beach, CA, United States, May 12-16, 2002, SAMPE, Covina, 2002, pp. 1862-1874.

[6] C. Ridgard, Out of autoclave composite technology for aerospace, defense and space structures, Proceedings of the SAMPE 2010 Spring Symposium (Eds. J.C. Fielding, S. Prybyla, L. Tate and S.W. Beckwith), Baltimore, MD, USA, May 18-21, 2009, SAMPE, Covina, 2009, Paper 218, pp. 1-11.

[7] S. Mortimer and M.J. Smith, Product development for out-of-autoclave (O.O.A.) manufacture of aerospace structure, Proceedings of the SAMPE 2010 Spring Symposium & Exhibition (Eds. R. Albers, P. Hubert and S.W. Beckwith), Seattle, WA, United States, May 17-20, 2010, SAMPE, Covina, 2010, Paper 379, pp. 1-11.

[8] C. Ridgard, Next generation out of autoclave systems, Proceedings of the SAMPE 2010 Spring Symposium & Exhibition (Eds. R. Albers, P. Hubert and S.W. Beckwith), Seattle, WA, United States, May 17-20, 2010, SAMPE, Covina, 2010, Paper 180, pp. 1-18.

[9] R. Stewart, New prepreg materials offer versatility, top performance, *Reinforced Plastics*, **53**, 2009, pp. 28-33 (doi: 10.1016/S0034-3617(09)70222-X).

[10] G. Gardiner, Resin-infused MS-21 wings and wingbox, *Composites World*, Gardner Business Media Inc., 2014, Cited May 13, 2015, Available: http://www.compositesworld.com/articles/resin-infused-ms-21-wings-and-wingbox.

[11] Y. Eom, L. Boogh, V. Michaud and J.a. Månson, A structure and property based process window for void free thermoset composites, *Polymer composites*, **22**, 2001, pp. 22-31 (doi: 10.1002/pc.10512).

[12] Y. Li, M. Li, Y. Gu and Z. Zhang, Numerical and experimental study on the effect of lay-up type and structural elements on thickness uniformity of L-shaped laminates, *Applied Composite Materials*, **16**, 2009, pp. 101-115 (doi: 10.1007/s10443-009-9080-z).

[13] X. Wang, Z. Zhang, F. Xie, M. Li, D. Dai and F. Wang, Correlated rules between complex structure of composite components and manufacturing defects in autoclave molding technology, *Journal of Reinforced Plastics and Composites*, **28**, 2009, pp. 2791-2803 (doi: 10.1177/0731684408093876).

[14] M. Brillant and P. Hubert, Modelling and characterization of thickness variations in L-shape out-of-autoclave laminates, *Proceedings of the SAMPE 2010 Spring Symposium and Exhibition*, *Long Beach, CA, United States*, *May 17-20*, *2010*, SAMPE, Covina, 2010, Paper 274, pp. 1-15.

[15] J. Cauberghs and P. Hubert, Effect of tight corners and ply terminations on quality in out-of-autoclave parts, *Proceedings of the SAMPE 2011 (Eds. V.P. Bailey, J.C. Leslie and S.W. Beckwith)*, *Long Beach, CA, United States*, *May 24-26*, *2011*, SAMPE, Covina, 2011, Paper 1271, pp. 1-15.

[16] T. Centea and P. Hubert, Out-of-autoclave prepreg consolidation under deficient pressure conditions, *Journal of Composite Materials*, **48**, 2014, pp. 2033-2045 (doi: 10.1177/0021998313494101).

[17] G.L. Hahn, G.G. Bond and J.H. Fogarty, Non-autoclave (prepreg) manufacturing technology: part scale-up with CYCOM 5320-1 prepregs, *Proceedings of the SAMPE 2011 Spring Symposium & Exhibition (Eds. V.P. Bailey, J.C. Leslie and S.W. Beckwith)*, *Long Beach, CA, USA*, *May 23-26*, *2011*, SAMPE, Covina, 2010, Paper 1139, pp. 1-15.

[18] A. Levy, J. Stadlin and P. Hubert, Corner consolidation in vacuum bag only processing of out-of-autoclave composite prepregs laminates, *Proceedings of the SAMPE 2014 Technical Conference*, *Seattle, WA, United States*, *June 2-5*, *2014*, SAMPE, Covina, 2014.

[19] S.M. Hughes, N. Krumenacker and P. Hubert, Out-of-autoclave prepreg processing: thermally assisted compaction of complex laminates, *Proceedings of the CANCOM 2015 International Conference on Composites*, *Edmonton, AB, Canada*, *August 18-20*, *2015*, Unpublished.

[20] P. Hubert and A. Poursartip, Aspects of the compaction of composite angle laminates: an experimental investigation, *Journal of Composite Materials*, **35**, 2001, pp. 2-26 (doi: 10.1177/002199801772661849).

[21] S.G. Lekhnitskii, Bending of plane anisotropic bars and curved beams, in *Anisotropic plates*, Gordon and Breach Science Publishers Inc., New York, 1968, pp. 57-114.

[22] K. Kedward, R. Wilson and S. McLean, Flexure of simply curved composite shapes, *Composites*, **20**, 1989, pp. 527-536 (doi: 10.1016/0010-4361(89)90911-7).

[23] W. Cui, T. Liu, J. Len and R. Ruo, Interlaminar tensile strength (ILTS) measurement of woven glass/polyester laminates using four-point curved beam specimen, Composites Part A: Applied Science and Manufacturing, 27, 1996, pp. 1097-1105 (doi: 10.1016/1359-835X(96)00071-1).

[24] ASTM standard D6415, 2006a (2013), Standard test method for measuring the curved beam strength of a fiber-reinforced polymer-matrix composite, ASTM International, 100 Bar Harbor Drive, West Conshohocken, PA 19428, United States, 2014 (doi: 10.1520/D6415_D6415M).

[25] J. Kratz, K. Hsiao, G. Fernlund and P. Hubert, Thermal models for MTM45-1 and Cycom 5320 out-of-autoclave prepreg resins, *Journal of Composite Materials*, **47**, 2013, pp. 341-352 (doi: 10.1177/0021998312440131).

[26] G. Seon, A. Makeev, Y. Nikishkov and E. Lee, Effects of defects on interlaminar tensile fatigue behavior of carbon/epoxy composites, *Composites Science and Technology*, **89**, 2013, pp. 194-201 (doi: 10.1016/j.compscitech.2013.10.006).